Influence of the nonlinear behavior of viscous dampers on the seismic demand hazard of building frames

(Article begins on next page)

15 February 2025

INFLUENCE OF THE NON LINEAR BEHAVIOUR OF VISCOUS DAMPERS ON THE SEISMIC DEMAND HAZARD OF BUILDING FRAMES

A. Dall'Asta[1], E. Tubaldi[1], L. Ragni[2]

[1]School of Architecture and Design, University of Camerino, Viale della Rimembranza, 63100 Ascoli Piceno (AP), Italy; E-mail: andrea.dallasta@unicam.it, etubaldi@gmail.com.

[2] Department of Civil and Building Engineering and Architecture, Polytechnic University of Marche, Via Brecce Bianche Ancona (AN), Italy; E-mail: laura.ragni@univpm.it.

SUMMARY

This paper analyzes the influence of damper properties on the probabilistic seismic performance of building frames equipped with viscous dampers. In particular, a probabilistic methodology is employed to evaluate the influence of the damper nonlinearity, measured by the damper exponent, on the performance of structural and non-structural components of building frames, as described by the response hazard curves of the relevant engineering demand parameters.

The performance variations due to changes in the damper nonlinearity level are evaluated and highlighted by considering two realistic design scenarios and by comparing the results of a set of cases involving dampers with different exponents designed to provide the same deterministic performance. By this way, it is possible to evaluate the influence of the nonlinear response and of its dispersion on the demand hazard. It is shown that the damper nonlinearity level strongly affects the seismic performance and different trends are observed for the demand parameters of interest. A comparison with code provisions shows that further investigation is necessary to provide more reliable design formulas accounting for the damping nonlinearity level.

INTRODUCTION

The extensive losses sustained by engineering systems during recent seismic events has highlighted the inadequacy of the seismic design based on the "life safety" or "collapse prevention" concept, and the need of controlling the seismic performance in terms of structural and non-structural damage at multiple hazard scenarios, as also suggested by recent Performance-Based Design (PBD) guidelines [1],[2],[3]. In this context, base isolation [4] or passive energy dissipation [5],[6] have emerged as effective technologies that permit to improve the seismic performance of new and existing buildings by significantly reducing the damage to both structural and non structural components.

Among passive energy dissipation systems, fluid viscous dampers proved to have some performance advantages since they permit to reduce both displacements and accelerations simultaneously [7],[8]. This can be very significant for those structures (e.g., hospitals or electrical stations) whose contents and components are sensitive to deformations or accelerations. Another property of viscous dampers that makes them preferable to other types of damper is related to their velocity-dependent behaviour, which implies large energy dissipation also at small deformation levels .

The response of viscous dampers is proportional to a power-law of the velocity and can be linear or nonlinear depending on the value of the velocity exponent α, usually varying in the range between 0.15 and 1 in structural engineering applications [9]. The earthquake response of building frames equipped with linear or nonlinear viscous dampers has been analyzed in many papers by using Single-Degree-Of-Freedom (SDOF) models [10],[11] as well as more complex structural models [8],[12][13]. In general, these studies observed that nonlinear viscous dampers permit to achieve the same displacement reduction as linear viscous dampers but with lower damper forces. Furthermore,

in the nonlinear case the damper forces do not increase significantly for velocities increasing beyond the design value, thus avoiding potential overload in the dampers and in the system to which they are connected [14][15].

Although all the above studies analyzed interesting aspects concerning the effectiveness of nonlinear viscous dampers in the design, they are all based on a "deterministic" measure of the seismic demand, i.e., they evaluate the seismic response by using a one-to-one relationship between the seismic intensity and a response parameters (usually coinciding with the mean response of a set of ground motions with a specific intensity level), and do not account for the response dispersion and the relevant effects on the structural reliability. The limits of this approach, currently employed in many seismic design guidelines [3],[16]-[18], have been highlighted in Bradley [19], who also stressed the importance of a more comprehensive performance assessment through probabilistic methodologies capable of fully accounting for the effect of the uncertainty of the seismic input.

Some recent works carried out the performance assessment of structural systems equipped with viscous dampers through probabilistic approaches in the framework of performance-based earthquake engineering (PBEE). For example, works [20]-[24] focused on probabilistic analysis of r.c. buildings retrofitted with linear viscous dampers [20] or steel moment resisting frames with linear viscous dampers [21]-[24]. These studies evaluated the seismic demand, in terms of inter-storey drift ratio as well as other response parameters relevant to the system performance, by accounting for the seismic input uncertainties. Other probabilistic studies [25],[26] were aimed at developing solution techniques for the optimal use of energy dissipating viscous dampers to minimize the life-cycle cost. However, these studies did not provide any insight on the effect of the nonlinear damper exponent. Some investigations on this effect were made by [27]-[29] but these studies are not in the context of PBEE and they were mainly oriented to develop simplified stochastic dynamic analysis procedures to evaluate the system response.

Since previously discussed deterministic studies on nonlinear dampers have highlighted that the velocity exponent α strongly influences the response of viscously damped structures, studies analyzing and comparing the probabilistic response of system equipped with both linear and non linear viscous dampers are a necessary step to evaluate the effective seismic performance of viscously damped structures and to measure the safety level properly. In particular, a deeper insight is required on very low velocity exponents, around 0.15-0.20, finding a growing interest in seismic applications. A first investigation on this topic has been recently carried out in [30][31] by employing a single-degree-of-freedom (SDOF) system. In particular, the study of Tubaldi et al. [30] has been developed within the PBEE framework. An extensive parametric analysis encompassing all the system characteristic (non-dimensional) parameters has been carried out by considering both kinematic and dynamic response quantities (relative displacement, absolute acceleration, damper force). The obtained results have shown that the dispersion of each of these response quantities induced by the seismic input variability differently changes by varying the parameter α. Moreover, results concerning a case study have shown the consequences of this effect on the structural safety, expressed in terms of risk of exceeding reference values of the response quantities of interest.

This paper focuses on the seismic reliability of multi-storey buildings equipped with viscous dampers, having in aim the evaluation of the influence of the damper nonlinearity, measured by α, on the performance of structural and non-structural components of the system. This performance is described in terms of response hazard curves, providing the mean annual frequency of exceedance of the response parameters of interest for the performance assessment and obtained by combining the information on both seismic hazard and seismic vulnerability.

The first part of the paper illustrates the probabilistic methodology employed to evaluate the influence of the exponent α on the performance, and the underlying assumptions. The second part reports the results of the application of the methodology to two multi-storey steel frames with different dynamic properties, selected from the SAC Phase II project and widely used in studies on seismic response control problems [21],[22],[32]. The performance variations due to changes in the damper nonlinearity level are evaluated and highlighted by considering a set of cases involving

dampers with different exponents α designed for the same deterministic performance objective at a reference seismic intensity. The probability distribution and the demand hazard of global response parameters (maximum inter-storey drift, maximum absolute acceleration, base shear) and of local response parameters (damper strokes and damper forces) are evaluated and discussed in a range of variation of annual frequency of exceedance spanning from service to ultimate limit states, considering a range of the nonlinear exponent spanning from 0.15 to 1.0. Finally, an assessment of the seismic performance obtained by employing the simplified formulas suggested by the seismic codes for the damper design is presented.

PROBABILISTIC SEISMIC PERFORMANCE ASSESSMENT OF FRAMES EQUIPPED WITH VISCOUS DAMPERS

Probabilistic framework for performance assessment

In the context of PBEE, the assessment of the seismic performance of a structural system can be carried out at different levels (e.g., by quantifying the seismic demand, the seismic damage, or the direct and indirect losses), and can encompass different sources of uncertainty affecting e.g. the earthquake input, the model parameters or the direct and indirect losses estimation [29]. In this study, the focus is on the seismic demand on the structural and non-structural components considering only the effects of the seismic input uncertainty, which usually provides the major effects. However, the same probabilistic framework can be used to include the effects of other sources of uncertainties, e.g. those affecting structural and damping parameters, on the performance assessment. This usually involves the application of simulation techniques, as shown in [25],[29],[33] or in [34]and [35] with reference to different passive seismic protection systems.

In PBEE, the ground motion uncertainty is usually described by separating the randomness in the input intensity, described by the intensity measure *IM* (capital letter denotes random variable), from the randomness in the record characteristics (record-to-record variability). The *IM* randomness is described by the hazard curve $v_{IM}(im)$, providing the mean annual frequency (MAF) of *IM* exceeding the value *im*, whereas the record-to-record variability is described by a representative ensemble of ground motions conditional on the considered *IM* level [19][36]. Different choices can be made for the *IM* and for the sets of records, which should be ideally representative of the seismic threat at the different *IM* levels [36][37].

The seismic demand can be monitored by a number of response parameters (engineering demand parameters *EDPs*) relevant to the performance assessment of the building. As for the case of the *IM*, the *EDP* variability can be described by the demand hazard curve $v_{EDP}(edp)$, providing the MAF of exceedance of a specific level of seismic demand *edp* and computed as:

$$v_{EDP}(edp) = \int_0^\infty P_{EDP|IM}(edp|im) \cdot |dv_{IM}(im)| \qquad (1)$$

where $P_{EDP|IM}(edp|im)$ denotes the probability that *EDP > edp* given *IM = im* and depends on the record-to-record variability of the response.

The probability $P_{EDP|IM}(edp|im)$ can be estimated at different *IM* levels by performing multi-stripe analysis (MSA) or incremental dynamic analysis [36]. These analyses consist in performing a series of simulations of the response of the structure subjected to a suite of input ground motions scaled to a common *IM* level, for different *IM* levels. A common assumption introduced in PBEE to simplify the assessment of $P_{EDP|IM}(edp|im)$ and to make possible some analytical calculations, is that the distribution of the demand conditional to the *IM* , $f_{EDP|IM}(edp|im)$, is lognormal. This assumption is appropriate also for the case of structural systems with nonlinear viscous dampers [30]. The lognormal distribution parameters $\mu_{\ln EDP|IM}(im)$ and $\sigma_{\ln EDP|IM}(im)$, the former denoting the

lognormal mean, and the latter the lognormal standard deviation (dispersion), can be evaluated from the response samples and they vary with the *IM* level considered [38].

It should be noted that although the derivation of the curve $v_{EDP}(edp)$ requires a specific *IM* be defined, the final demand hazard should be independent of this choice [19].

In the following, the term *deterministic demand* denotes the mean value $\mu_{EDP|IM}(im)$ measured for a set of seismic inputs with the same intensity *im* [19]. The term "deterministic" underlines that there is a one-to-one relationship between the seismic input and the structural demand and information about the dispersion of the response is not considered. In this context, the MAF of exceedance of the deterministic demand coincides with $v_{IM}(im)$. It is also observed that this demand evaluation depends on the particular *IM* considered [19].

Methodology for the seismic performance assessment of frames equipped with viscous dampers

This section illustrates the methodology developed to evaluate the influence of the damper nonlinearity on the performance of frames equipped with viscous dampers and to evaluate the differences between the seismic demand evaluated by the deterministic and the probabilistic approach. The comparison is performed by considering families of case studies designed to achieve the same deterministic seismic performance but involving dampers with different values of the nonlinear parameter α. Each family concerns a specific design scenario, described by the seismic hazard and the dynamical properties of the frames. The methodology is articulated into three-stages, described as follows.

1. Damper design

The viscous dampers design is carried out by assigning the damper properties, i.e., the exponent α and the viscous constants c_{di} at the *i*-th storey. A deterministic performance objective is sought consistently with modern seismic codes. The design objective corresponds to achieving a target mean value of IDR_{max}, the maximum peak inter-storey drift among the various storeys, for the set of records scaled to a reference intensity level im_{ref}, with relevant exceedance rate $v_{IM}(im_{ref}) = v_{ref}$. For example, v_{ref} can be taken equal to 0.0021, corresponding to a 10% probability of exceedance in 50 years, which is the probability value associated to the ultimate limit state (ULS) according to EC8 [3]. The design procedure is applied by considering different levels of damper nonlinearity, described by the exponent α, and yields a distribution of dampers at storeys providing the chosen performance objective.

2. Assessment of the influence of damper nonlinearity on the demand hazard.

In the second stage of the methodology, multi-stripe analysis [36] is performed to estimate, for the different levels of the dampers nonlinearity, the samples that define the statistical distribution of the *EDP*s of interest for the performance assessment.

In the following study different (global and local) *EDP*s will be considered: a) the maximum inter-storey drift along the building height, IDR_{max}; the maximum floor acceleration along the building height, A_{max}; c) the base shear, V_b; d) the stroke $D_{d,i}$ of the *i*-th damper; e) the force $F_{d,i}$ of the *i*-th damper. It is understood that these demand parameters are the maximum values observed during the time history.

The parameters IDR_{max} and A_{max} describe the performance of the structural and non-structural (displacement-sensitive and acceleration-sensitive) components, V_b describes the forces impaired on the foundations, resulting from the sum of the shear of the base columns and of the horizontal force of the dampers at the base storey. The other two *EDP*s are local parameters that permit to monitor the damper performance, which is controlled by both the force and the stroke demand. These

quantities usually vary from damper to damper and have a non uniform distribution along the building height.

The parameters $\mu_{\ln EDP|IM}(im)$ and $\sigma_{\ln EDP|IM}(im)$ that define the lognormally-distributed demand are estimated based on the response samples by using common statistical inference tools as already described in Tubaldi et al. [30]. It is noteworthy that in the case of a lognormal distribution, the relation between the mean response $\mu_{EDP|IM}(im)$, adopted in the deterministic approach, the lognormal mean $\mu_{\ln EDP|IM}(im)$ and lognormal standard deviation $\sigma_{\ln EDP|IM}(im)$ is:

$$\mu_{EDP|IM}(im) = \exp\left[\mu_{\ln EDP|IM}(im) + \frac{1}{2}\sigma_{\ln EDP|IM}^2(im)\right] \tag{2}$$

Also the response percentiles can be easily evaluated once the distribution parameters have been calculated.

The response hazard curves for the different *EDP*s are derived based on Eqn. (1). They can be directly used to evaluate the effect of the dampers on the MAF of exceedance of predefined response thresholds and also provide the basis for comparing the solutions corresponding to different levels of damper nonlinearity.

3. Comparison of probabilistic and deterministic approach for the performance assessment.

The two approaches for the seismic demand assessment are compared by considering the probabilistic demand measure $edp(v)$, obtained as the inverse function of the demand hazard curve and representing the demand value with a MAF of exceedance equal to *v*, and the deterministic demand measure $\mu_{EDP|IM}(im_{ref})$, representing the mean demand at the reference seismic intensity level with MAF of exceedance v_{ref}.

The probabilistic and deterministic demand measures change with the damper nonlinearity level α and their ratio, defined as:

$$R_{EDP}(v,\alpha) = \frac{edp(v,\alpha)}{\mu_{EDP|IM}(im_{ref},\alpha)} \tag{3}$$

can be interpreted as the multiplication factor to be applied to $\mu_{EDP|IM}(im_{ref},\alpha)$ to obtain the demand with a MAF of exceedance equal to *v*.

The influence of α on the ratio $R_{EDP}(v,\alpha)$ for the different *EDP*s of interest is evaluated by considering values of *v* between 10^{-2} and 10^{-5} in order to investigate wide ranges of target seismic performance levels. The lower and upper bounds have been chosen based on the target failure rates specified in seismic codes for the serviceability and the collapse limit state [39],[40].

PROBABILISTIC ANALYSES RESULTS

Benchmark structures and hazard scenario

The two analysed structures are a 3 -storey and a 9-storey steel moment-resisting frame buildings (Fig. 1) designed as part of the SAC steel project and located in the same site in the Los Angeles area. The two buildings significantly differ in their dynamic properties and strength capacity under horizontal forces. Their structures were designed in compliance with local code requirements and design practices for office building, by considering the gravity, wind, and seismic load. The structural system for both the buildings consists of steel perimeter moment frames and interior

gravity frames with shear connections. Detailed descriptions of these structures, including dimensions and member sizes, are provided in many other works [22].
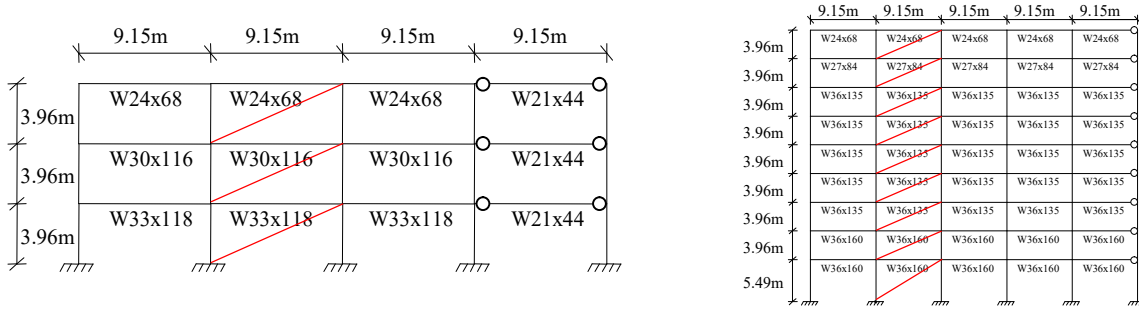

Fig. 1. Building model description and properties: a) three-storey frame, b) nine-storey frame.

The structural models are developed in Opensees [41] by adopting the general criteria used in [22],[32]. The structures are modelled as two-dimensional frames describing half of the symmetric buildings in the north–south direction. The inelastic members behaviour has been described by using distributed plasticity fiber element models with nonlinear material properties. The nonlinear geometrical effects induced by the vertical loads acting on both the interior frames and the modelled frame are included in the analysis by employing an elastic P-delta column with high axial stiffness and negligible bending stiffness, so that it does not contribute to resist the seismic induced loads. The floor vertical loads are assigned to this column at each floor level and a corotational formulation is used to capture the nonlinear geometrical effects.

The damping properties inherent to the behaviour of the steel frames within the elastic range are described by using the Rayleigh damping model, whose parameters have been calibrated by assuming a 2% damping factor for the first two vibration modes. Table 1 reports the relevant modal properties of the 3- and 9-storey structures, i.e., the vibration periods, T_i, and the mass participation factors (normalized by the total mass), MPF_i, of the first three modes. The observed vibration periods are in close agreement with those reported in [22] and in [32].

Table 1. Modal properties of the 3- and 9-storey frames.

Study case	mode	T_i	MPF_i
	1	0.999	0.828
3-storey	2	0.325	0.137
	3	0.175	0.037
	1	2.225	0.828
9-storey	2	0.836	0.109
	3	0.481	0.038

Fig. 2 reports the capacity curves of the frames, obtained through pushover analysis by considering a lateral load patter proportional to the first modal shape. These curves are in good agreement with the corresponding curves reported in [22].
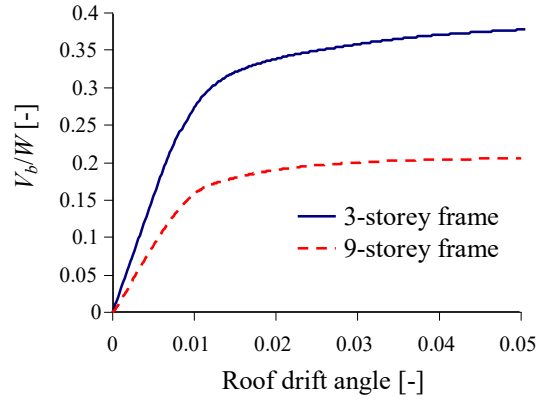
Fig. 2. Capacity curves of the frames expressed in terms of base shear normalized by the self weight V_b/W and roof drift angle (top displacement divided by the height).

The seismic intensity IM is described by the spectral pseudo-acceleration $S_a(T_1,2\%)$ of a linear elastic SDOF system with 2% damping ratio and fundamental vibration period equal to that of the structure T_1 [22]. This IM has been chosen because it represents the basis of the current seismic hazard maps and building code practice [19]. The choice of this IM is also driven by the aim of this study to evaluate the safety levels achieved by employing a "deterministic approach" for the dampers design consistent with modern seismic codes [16], which employ a response spectrum to define the seismic input. The hazard curves corresponding to the chosen IM, for the three storey and the nine storey building frames, are reported in Fig. 3 and are taken from [22]. They are in the form $v_{IM}(im) = k_0 im^{-k_1}$, where $k_0 = 0.00142$ and $k_1 = 3.25$ for the 3-storey frame, and $k_0 = 0.000262$ and $k_1 = 2.08$ for the 9-storey frame. In Fig. 3, the intensity levels corresponding to a probability of exceedance of 2%, 10% and 50% in 50yrs are also highlighted. These are the intensity levels considered for the assessment of the frames according to the codes. The case studies will be designed by considering the MAF of exceedance $v_{ref} = v_{IM}(im_{ref}) = 0.0021$ (probability of exceedance of 10% in 50 years), associated to the intensities $im_{ref} = 0.8866g$ for the 3-storey frame, and $im_{ref} = 0.3676g$ for the 9-storey frame (g is the gravity acceleration).

The record-to-record variability has been described by employing ground motions taken from the set of 60 records used in the SAC project, whose characteristics are reported in Barroso [21]. These records are characterized by different seismic intensities, frequency content, and duration. For each IM level covered in the multi-stripe analysis [36], the 30 ground motions with the closest IM values have been selected and scaled to that IM level. This approach, yielding different ground motion combinations for the different IM levels considered, permits to avoid excessive scaling of the records.
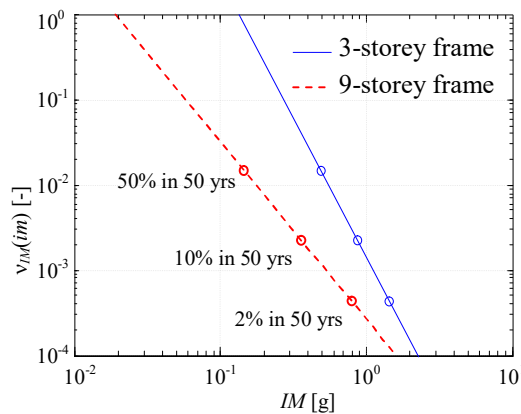

Fig. 3. Hazard curve for (a) the three storey and (b) the nine storey building frames.

The relation between the seismic input and the dynamic properties of the case studies is illustrated in Fig. 4, where the pseudo-acceleration response spectra of the 30 records representative of the earthquake input at $IM = im_{ref}$ are reported together with the mean response spectrum. In the same figure, the spectral values at the first three vibration periods are also reported by circles. The 9-storey case is more flexible than the 3-storey case and it is worth to observe that the ratio between the spectral ordinates at higher periods and at the first period of vibration is higher for the 9-storey frame than for the 3-storey frame. Thus the latter frame is expected to be more sensitive to the higher mode contributions.

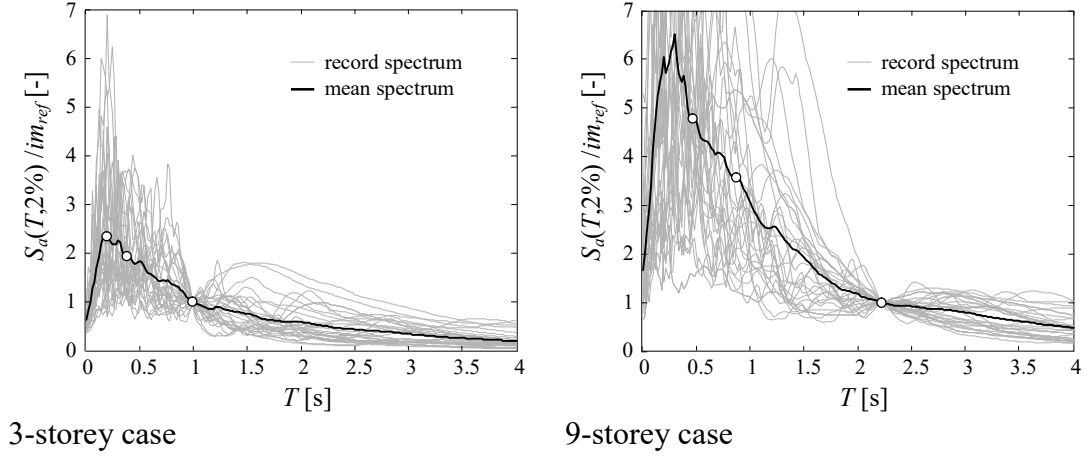3-storey case   9-storey case

Fig. 4. Pseudo-acceleration response spectra of the records at im_{ref} for the three-storey (a) and the nine-storey frame (b).

The set of solutions with added damping have been generated by requiring the same target mean value of IDR_{max}, $\mu_{IDR|IM}\left(im_{ref}\right)$ at $IM = im_{ref}$ for the frames equipped with the dampers characterized by different nonlinearity levels. The starting values of $\mu_{IDR|IM}\left(im_{ref}\right)$ for the bare frames are 2.80% for the 3-storey case and 2.41% for the 9-storey case. The target values of $\mu_{IDR|IM}\left(im_{ref}\right)$ are equal to 1.20% for the 3-storey frame and 1.07% for the 9-storey frame, and they have been chosen to provide an additional damping ratio of exactly 30% to the first mode in the linear case ($\alpha = 1$). The corresponding demand reduction is of about 55% for both the 3-storey and 9-storey case.

It is noteworthy that there are different distributions of damper properties along the building height that provide the same added damping ratio at the first mode. Therefore, the determination of the viscous constants c_{di} is arbitrary and standard methods as well as more advanced methods based on optimization procedures can be used (see [42][43]for an overview of the damping placement methods as well as a comparison in terms of performances). Standard methods include the most simple distribution characterized by the same damping constant c_d at each storey, or distributions where the damping constants are proportional to the storey stiffness or shear, this latter usually leading to larger dampers at the lower storeys. Differently, advanced methods aim at finding the optimal damper distribution by employing different optimisation algorithms (i.e. sequential search algorithms, mathematic programming algorithms or genetic algorithms) and by considering different performance objectives (e.g. inter-storey drift, absolute acceleration or damper forces). Recently, studies on multi-objective optimization [7] or optimization methods accounting for different seismicity levels [14] [25] are also developed. In general, the optimal design solution changes by changing the optimization method adopted, thus a standard placement methods is considered in this paper. Since the differences observed among standard methods are usually not very large [42], in this study a uniform distribution is assumed for its simplicity and effectiveness. Table 2 reports the set of design solutions corresponding to the different values of α for the two

frames considered. Fig. 5 shows that these solutions lead, for the different α values considered, to mean values of the inter-storey drift demand uniformly distributed in the 3-storey case, and decreasing along the building height in the 9-storey case.

Table 2. Damper design parameters for different levels of damper nonlinearity.

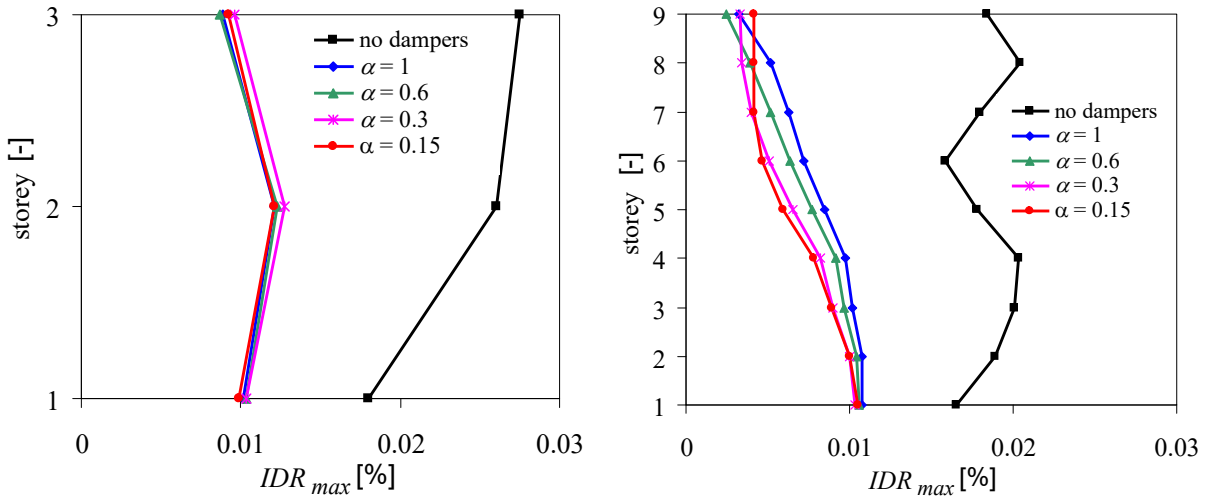| Case study	α	c_d [kNs$^\alpha$/m$^\alpha$]	Case study	α	c_d [kNs$^\alpha$/m$^\alpha$]
3-storey	1	10200	9-storey	1	35750
	0.6	5150		0.6	15500
	0.3	2800		0.3	9900
	0.15	2300		0.15	8500

Fig. 5. Distribution of the inter-storey drift demands for the 3-storey case (a) and the 9-storey case (b).

*Probabilistic response and seismic demand hazard curves*

This section analyzes the influence of the damper nonlinearity on the seismic response variability and on the seismic demand hazard of the case studies. The variability of the response at different intensity levels is described synthetically by the median, 84th and 16th percentiles of the *EDPs* relevant to the performance assessment (Fig. 6a-e for the 3-storey case, Fig. 8a-e for the 9-storey case), whereas the influence of the nonlinear parameter α on the seismic demand hazard is analyzed by comparing the corresponding demand hazard curves $v_{EDP}(edp)$ (Fig. 6f-j for the 3-storey case, Fig. 8f-j for the 9-sterey case), providing the MAF of exceedance of each response parameter. The reported plots refer to the two extreme values of the damper exponents, $\alpha = 0.15$ and $\alpha = 1$. The dotted lines are located at the reference seismic intensity im_{ref} and at the corresponding MAF of exceedance v_{ref}.

For what concerns the 3-storey case, it can be observed that the dampers are more effective in reducing the system inter-storey drifts in the nonlinear case than in the linear case for seismic intensities lower than im_{ref}, whereas they control worse these drifts for larger seismic intensities. In fact, the median value of IDR_{max} is lower in the nonlinear case than in the linear case for low *IM* values, and becomes higher for high *IM* values (Fig. 6a). Moreover, the variance increases with the seismic intensity and it is higher in the nonlinear case. Consequently, the MAF of exceedance of the inter-storey drift demand is lower in the nonlinear case than in the linear case for low IDR_{max} values, and higher for high IDR_{max} values (Fig. 6f). The two demand hazard curves intersect at approximately the design target IDR_{max} value, i.e., 1.20%.

Differently, the median value of the maximum absolute acceleration A_{max}, as well its variance, is higher in the system with nonlinear dampers than in the system with linear dampers at all the intensity levels (Fig. 6c). As a consequence, the values of the MAF of exceedance of A_{max} are always higher in the nonlinear case than in the linear case (Fig. 6g).

Strokes $D_{d,i}$ and forces $F_{d,i}$ of the dampers are local parameters exhibiting statistics which usually differ from storey to storey and they show a different sensitivity to the seismic input variability [44],[45]. In order to compare results coming from different dampers it is necessary to normalize their *EDP*s. In the following the reported values of the strokes and of the forces are normalized storey by storey by dividing them by the deterministic demand value at the reference seismic intensity. The normalized strokes and forces are denoted as $\Delta_{d,i}$ and $\psi_{d,i}$, respectively. A synthetic information is reported by plotting the statistics and the demand hazard curves of the maximum (normalized) values observed among the storeys, denoted as $\Delta_{d,max}$ and $\psi_{d,max}$.

The global trend of the maximum (normalized) stroke is similar to the trend of IDR_{max} even if the two quantities may attain their maxima at different storeys. However, differently from the results relevant to IDR_{max} , the demand hazard curves for $\Delta_{d,max}$ in the linear and nonlinear case assume very different values in correspondence of the reference MAF of exceedance (ν_{ref}). On the other hand, the maximum normalized damper forces $\psi_{d,max}$ (Fig. 6d) show an opposite trend. In fact, since in the non linear case the damper forces increase less and less as the velocity increases, the median value of $\psi_{d,max}$ is larger in the nonlinear case than in the linear case for low *IM* values and becomes significantly lower at high *IM* values. Moreover, the dispersion is low at all the *IM* levels in both the linear and nonlinear case. The combined effect of the small dispersion and of the moderate variation of the mean value of $\psi_{d,max}$ results in a force demand in the nonlinear case that increases only slightly by reducing the MAF of exceedance, while very larger variations occur in the linear case (Fig. 6i). Consequently, the two hazard curves intersect one with the other, and the values of $\psi_{d,max}$ are lower in the linear case than in the nonlinear case for high ν values, and higher for low ν values. Similar effects of the damper nonlinearity for seismic intensities higher or lower than the one employed to evaluate the design dampers stroke and force have been observed in the previous study of the authors [30] with reference to a SDOF system. Analogous results were also reported in [14], though this study is based on a different (deterministic) approach and includes only two seismicity levels.
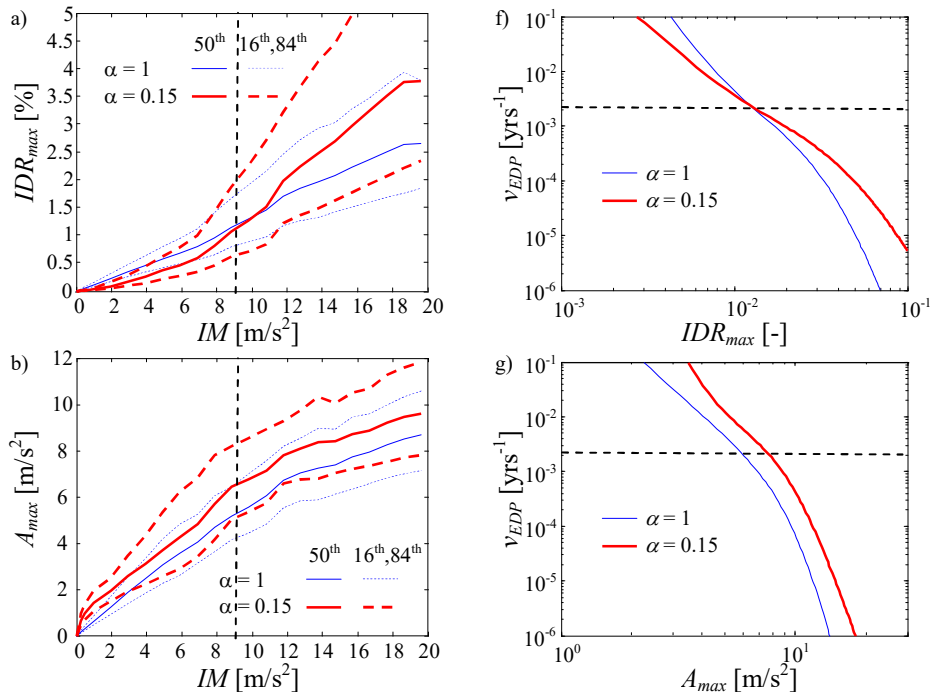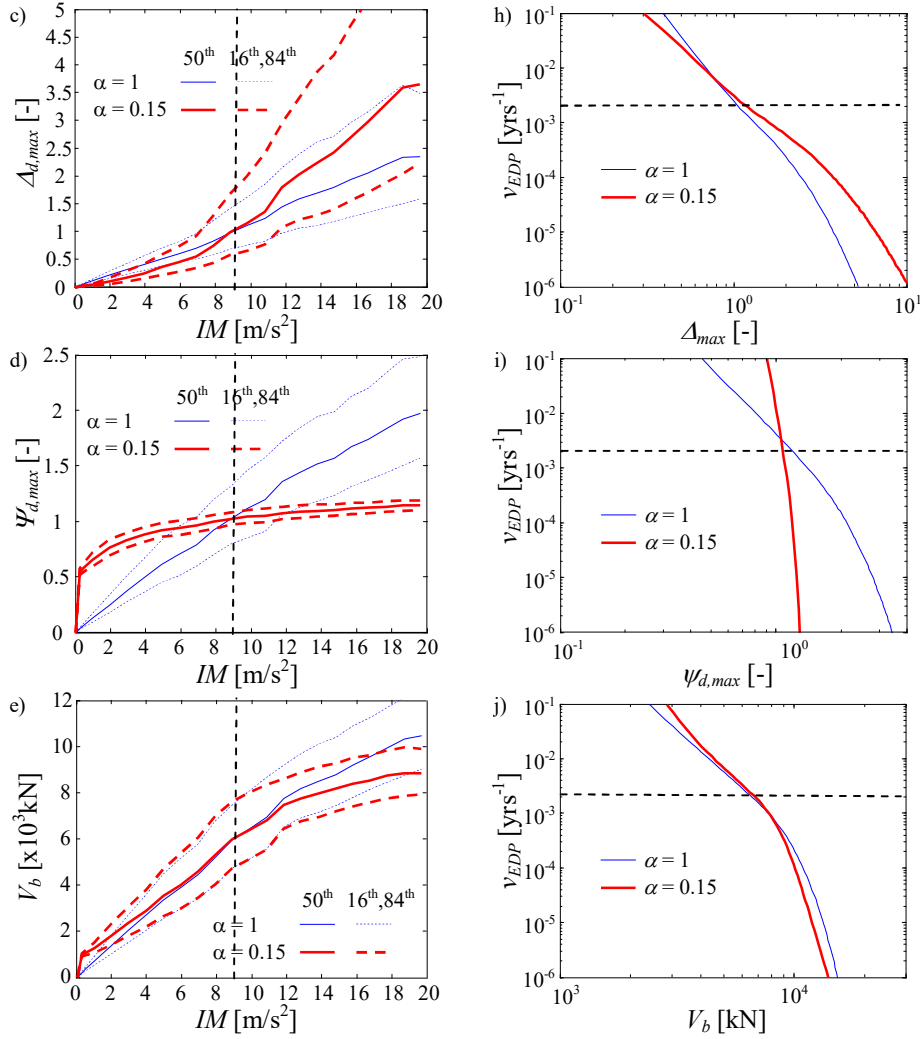
Fig. 6. Response statistics for the 3-storey frame corresponding to the dampers nonlinearity levels $\alpha=1$ and $\alpha=0.15$: 50th, 16th and 84th percentiles vs. *IM* (a-e), and response hazard curves (f-j) .

Finally, the median values and dispersions of the base shear V_b in the linear and nonlinear case are very similar to each other for all the seismic intensity levels considered (Fig. 6e), despite the damper forces show very different trends. As expected, also the base shear hazard curves are almost overlapping (Fig. 6j). At this regard it is useful to remind that the base shear V_b results from two, non synchronous, contributions due to the frame (base column shear V_s) and the dissipative bracings (horizontal components of the base damper forces V_d). In order to investigate separately these two contributions, the values of V_d and of V_s are plotted vs. *IM* in Fig. 7. It can be observed that while the median values of V_s are similar in the linear and non linear case, the variance is larger for the non linear case, due to the already observed large variance affecting the structure displacements. On the other hand, the contribution of the dampers has a very different trend. In particular, in the linear case the values of V_d are always lower than the values of V_s, while the value of total base shear is lower than the sum of the two contributions since these are not synchronous. Moreover, the variance of the dampers contribution is similar to the variance of the frame contribution, thus the two system components both contribute to the variance of the total base shear. Differently, in the nonlinear case the median values of V_d are higher than the median values of V_s for very low *IM* levels and become significantly lower at high *IM* levels, since the base damper force cannot increase appreciably for vary low values of α. In this case, the median value of the total base shear is close to the sum of the contributions of the two system components, confirming that the out-of-phase effect is lost with small α values as already observed in other papers (e.g. [14]). Moreover, as already discussed for the maximum normalized damper force, the variance of the damper

contribution to the base shear is very limited, thus the frame mainly contributes to the variance of the total base shear. In conclusion, even if the statistics of the total base shear do not change significantly with α, the two single contributions of the frame and of the dampers show very different characteristics, and this can differently influence the demand hazard and the design of the two system components.
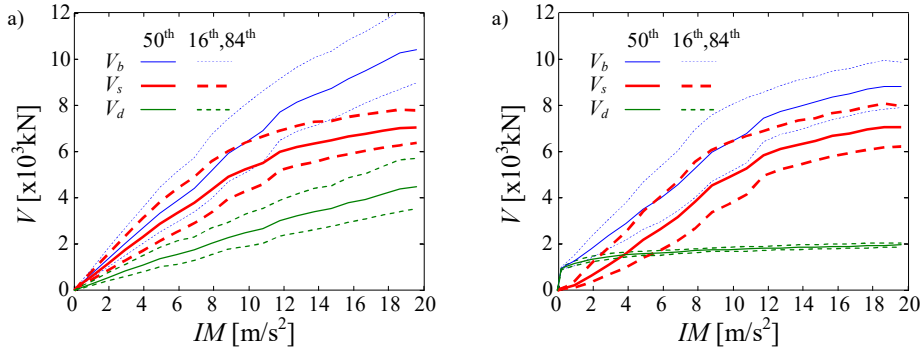

Fig. 7. Variation with *IM* of total base shear, frame base shear and dampers base shear for the 3-storey frame in the case of linear dampers (a) and of nonlinear dampers (b).

Fig. 8 collects the results concerning the 9-storey frame, characterized by a seismic hazard and modal properties different from those of the 3-storey frame.

The trends followed by IDR_{max} are approximately similar to those observed for the 3-storey frame. However, in the nonlinear case, the values of the dispersion observed for low (i.e., more probable) seismic levels are larger and this expands the range of demand values where the nonlinear MAF of exceedance is higher than the linear one.

The results about the maximum acceleration are similar to those observed for the 3-storey case. In fact, the median values of A_{max} are always higher in the nonlinear case than in the linear case, the dispersion are comparable and the MAF of exceedance in the nonlinear case is always higher than the corresponding MAF of exceedance in the linear case.

Also the trends of the maximum normalized damper strokes and forces follow trends similar to those observed for the 3-storey frame; however, in the 9-storey frame the stroke demand in the nonlinear case is larger than the demand in the linear case for all the spanned values of v.

Finally, the differences in the base shear demand observed between the linear and nonlinear case are more significant for the 9-storey frame with respect to the 3.storey frame. This can be explained by observing and comparing the contributions to the base shear from the dampers and from the frame (Fig. 9). In fact, compared to the case of the 3-storey frame (Fig. 7), V_d assumes very high values, which are even higher than the values of V_s at high *IM* levels in the linear case. This is the result of the high flexibility of the frame and the high influence of the contribution of higher order modes to the damper forces [46][47]. Consequently, the total base shear is significantly influenced by the damper forces and this also explains why the trend of the hazard curves of the base shear is more similar to the trend of the damper forces in the case of 9-storeys frame than 3-storeys frame.
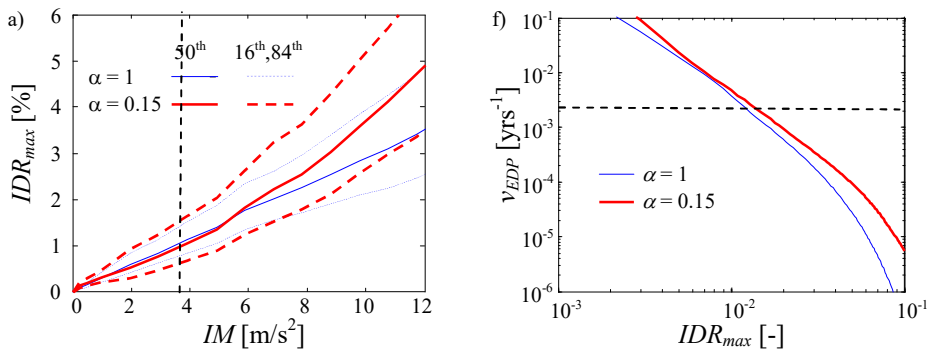
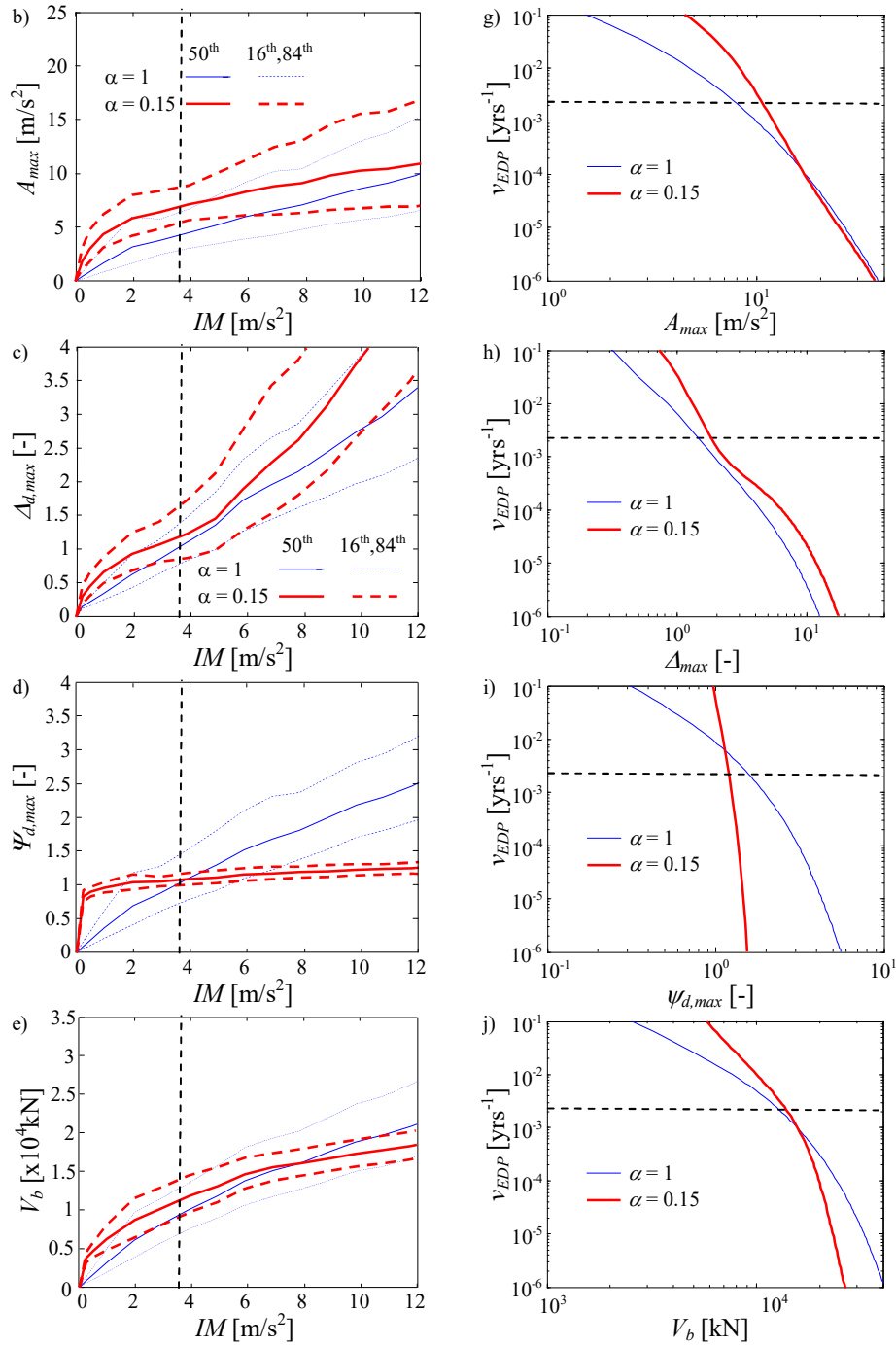Fig. 8. Response statistics for the 9-storey frame corresponding to the dampers nonlinearity levels $\alpha=1$ and $\alpha=0.15$: 50th, 16th and 84th percentiles vs. *IM* (a-e), and response hazard curves (f-j).
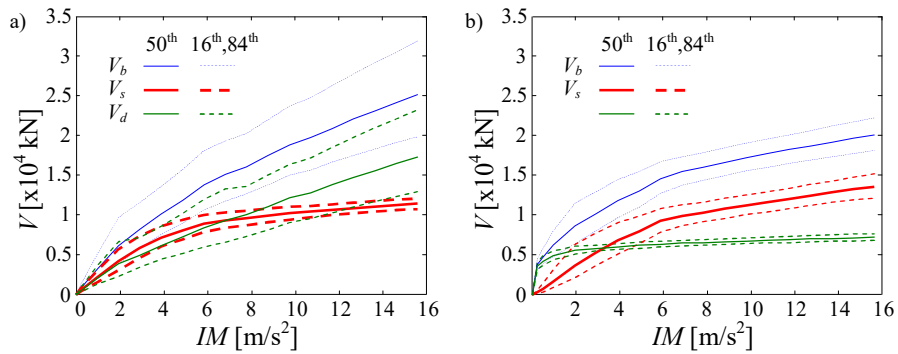

Fig. 9. Variation with *IM* of total base shear, frame base shear and dampers base shear in the case of linear dampers (a) and of nonlinear dampers (b).

Deterministic vs. probabilistic performance assessment at the reference MAF of exceedance

In order to compare and quantify the differences between the deterministic approach and the probabilistic approach at the reference condition considered for the design, the demand ratios $R_{EDP}(v)$, defined by Eqn. (3), are numerically evaluated for the different response parameters of interest at $v = v_{ref}$, for both the 3-storey and the 9-storey frame. In this case, the ratios $R_{EDP}(v_{ref})$ provide a comparison between the demand evaluated through the probabilistic approach for a MAF of exceedance v_{ref} (see Fig. 6f-j for the 3-storey case, Fig. 8f-j for the 9-sterey case) and the demand $\mu_{EDP|IM}(im_{ref})$ resulting from the deterministic approach [19]. It is noteworthy that the smaller the response dispersion, the closer the ratio $R_{EDP}(v_{ref})$ gets to 1.

The observed values of $R_{EDP}(v_{ref})$ are reported in Table 3. As a general consideration, the combined effect of the trends of the *edp* dispersion and of the seismic hazard curve $v_{IM}(im)$ provides values of $R_{EDP}(v_{ref})$ larger than 1. Thus, the actual demand value with an exceedance rate of v_{ref} is always larger than the corresponding mean demand value employed in the deterministic performance assessment. It is also worth to observe that the values of $R_{EDP}(v_{ref})$ differ significantly for the various response parameters and they also change significantly by varying α.

In general, the values observed in the 3-storey case, spanning the range 1.040-1.187, are lower than corresponding values observed in the 9-storey case, spanning the range 1.114-1.735. This difference is mainly due to the response variability associated to the higher vibration modes, that is more notable in the 9-storey case, as previously discussed in commenting Fig.4.

The analysis of the linear case results ($\alpha = 1$) shows that the values of $R_{EDP}(v_{ref})$ relevant to dynamic quantities, as the maximum damper forces and the maximum absolute storey accelerations, are larger than the values observed for kinematic quantities, as the maximum inter-storey drift and damper strokes, coherently with the *edp* response dispersions observed in the previous section in the neighbourhood of the reference seismic intensity (see Figs.5-7). Intermediate results are obtained for the base shear and this is due to the combined effects of the stiffness contribution, proportional to the deformation, and the contribution provided by the damper forces.

The variation of the $R_{EDP}(v_{ref})$ value with α exhibits a trend coherent with that of the response variability: moving from the linear case $\alpha = 1$ toward the nonlinear case $\alpha = 0.15$ the dispersions and consequently the $R_{EDP}(v_{ref})$ values increase in the case of the maximum inter-storey drift and damper strokes, whereas an opposite situation is observed for the damper forces. A less evident decreasing trend is observed for the storey absolute accelerations. The variation in the base shear are generally very low, in consequence of the opposite trends of the deformation-dependent contribution and of the viscous force-dependent contribution.

The differences observed between the demand measure obtained through the probabilistic approach and the conventional deterministic demand expressed by the mean value $\mu_{EDP|IM}(im_{ref})$ are notable for the considered case studies (up to 75% for accelerations, 45% for forces and 33% for inter-storey drifts). It is noteworthy that different results and trends may be observed by changing the damper distribution, i.e. by adopting different standard distributions or optimal distributions resulting from the application of optimization methods ([7],[14],[25],[42][43]). Nevertheless, the results reported in this study are interesting because they show the relevance of the problem and suggest the need for further investigations, encompassing different damper distributions as well as a wider range of damping levels, structural properties and seismic input characteristics.

Table 3. Ratios $R_{EDP}(v_{ref})$ for the different *EDP*s and the 3- and 9-storey frames.

3-storey frame					9-storey frame				
α	0.15	0.3	0.6	1	α	0.15	0.3	0.6	1
IDR$_{max}$	1.067	1.052	1.051	1.054	IDR$_{max}$	1.327	1.289	1.225	1.138
A$_{max}$	1.163	1.187	1.171	1.126	A$_{max}$	1.503	1.529	1.735	1.735
Δ$_{d,max}$	1.066	1.042	1.040	1.051	Δ$_{d,max}$	1.275	1.202	1.224	1.197
Ψ$_{d,max}$	1.047	1.074	1.110	1.129	Ψ$_{d,max}$	1.114	1.208	1.373	1.451
V$_b$	1.102	1.100	1.096	1.085	V$_b$	1.207	1.248	1.293	1.301

Relationship between demand and MAF of exceedance

This section analyzes the relationships between the MAFs of exceedance and the EDPs, having in aim to compare the trends of the different demand parameters and to evaluate the influence of the nonlinear damper parameter α. Presented results span the range of MAFs from 10^{-2} to 10^{-5} which are relevant for the service and ultimate limit states [40]. The values of the parameter α considered are: 0.15, 0.30, 0.60, and 1.00.

Fig. 10 shows the variation with v of the ratio $R_{EDP}(v)$ for the 3-storey case (Fig. 10a-e), and for the 9-storey case (Fig. 10f-j). The values of $R_{EDP}(v)$ increase by increasing v, as expected, but with different trends for the various response parameters and values of α considered in this study .

The demand concerning the displacements, as the maximum inter-storey drifts and damper strokes, generally show larger increments by increasing the MAF of exceedance when the nonlinear parameter α decreases while an opposite trend can be observed for the dynamic quantities, as the absolute accelerations at storeys, the damper forces and the base shear. The 3-storey case and the 9-storey case qualitatively show the same trends, even if the variations concerning the damper forces and the base shear are enhanced in the 9-storey case.

It is interesting to analyze the shape of the relationships between the demand and the natural logarithm of the MAF of exceedance. This relationship is essentially linear for the damper forces, for all the values of the parameter α and for both the frames. Its slope strongly depends on the nonlinear parameter α. Differently, the law is always less than linearly proportional for the base shear whereas it is more than linearly proportional for the displacements, damper strokes and accelerations. Also in this case, the slopes depend on the nonlinear behaviour of the dampers.

These results can be used to check approximate formulas used in practical design and an example is discussed in the next section by considering FEMA provisions.
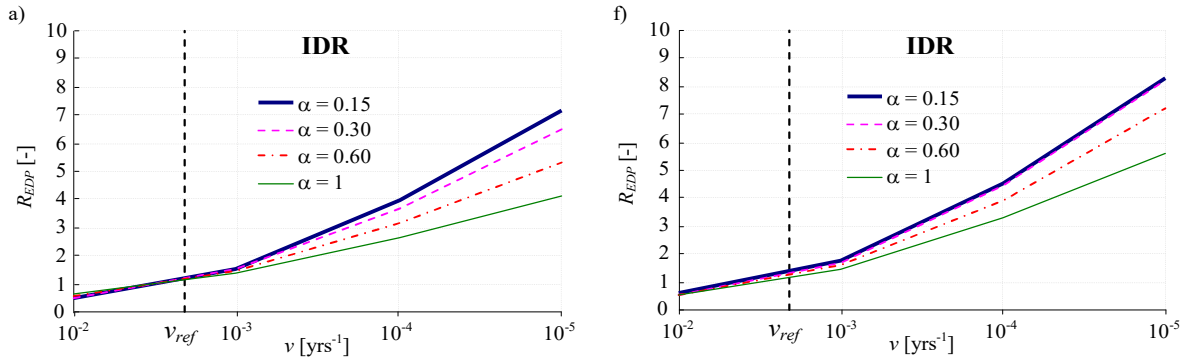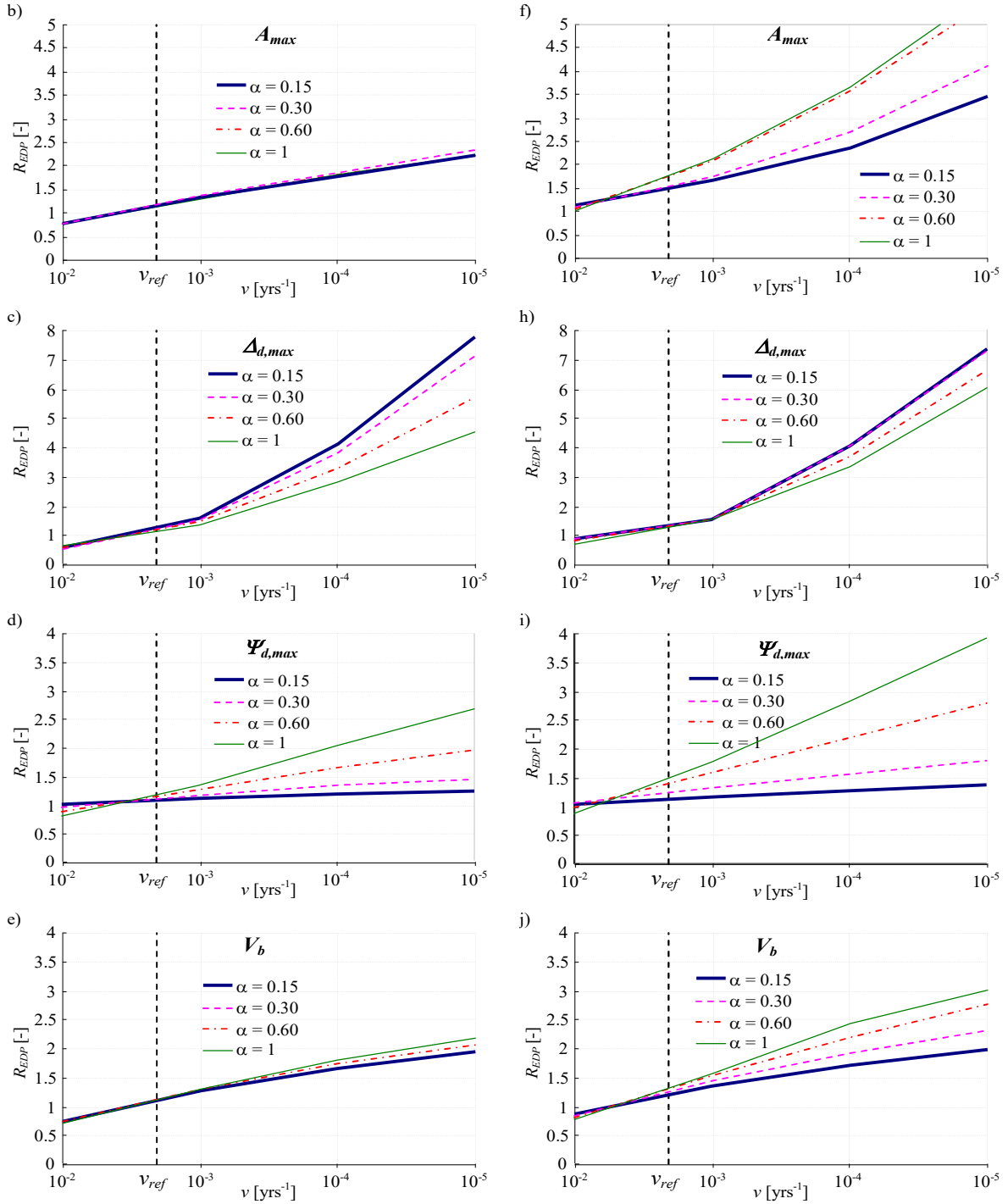
Fig. 10. Variation with the target MAF level v of $R_{EDP}(v)$ for the 3-storey case (a-e) and for the 9-storey case (f-j).

Damper statistics and reliability levels provided by simplified formulas

In this section, the MAF of exceedance of the demand provided by current code prescriptions for the damper design is evaluated by employing the hazard curves and the relationships between demand and MAFs of exceedance discussed in the previous sections.

According to ASCE 41-06 [2], velocity-dependent dissipation devices shall be capable of sustaining displacements equal to 200% of the maximum displacement calculated for earthquakes intensities with a 2% probability of being exceeded in 50 years. Velocity-dependent devices should also sustain the forces associated to velocities calculated for the same earthquake intensity and amplified by the same factor. The 200% factor reduces to 130% if at least four devices are provided at a given storey.

The aim of this type of provisions is to extrapolate a conventional value of the demand with a MAF of exceedance suitable for a reliability assessment by starting from the seismic demand obtained from the structural analysis. This should permit to perform a reliability assessment by a direct comparison between the conventional values of the demand and the capacity [40].

Table 4 and Table 5 report and compare the results of this assessment for the case of linear dampers ($\alpha = 1.00$) and of nonlinear dampers with $\alpha = 0.15$. They report the code design values of the damper stroke D_d and forces F_d at the various storeys of the 3-storey and 9-storey frame, obtained by amplifying strokes and damper velocities (calculated for earthquakes intensities with a 2% probability of being exceeded in 50 years) with a factor of 130% (Table 4) and of 200% (Table 5). Tables also report the MAFs of exceedance of the design (amplified) values deduced from the hazard curves and the ratios r_D and r_F between these MAFs of exceedance and the MAFs of exceedance corresponding to the reference (not amplified) values of strokes D_0 and forces F_0. For each case also the maximum values of the ratios r_D and r_F are reported. The more the approximated approach based on amplification factors is effective, the more the ratio values of r_D and r_F are similar.

With reference to the linear behaviour, it can be observed that ratios r_D and r_F of the 3-storey case are roughly uniform throughout the storeys for both the strokes and the forces but the values observed for the force are significantly lower than the values observed for the strokes. The MAFs of exceedance of the magnified strokes D_d are equal or lower than 42% of the MAFs of exceedance of the reference value D_0 while the values concerning the damper forces reduce to 23% or more.

In the case of the 9-storey frame with linear dampers, the MAFs of exceedance show a similar trend but the values measured for the forces are less regularly distributed along the building height and their maximum is higher.

By passing from the linear case to the nonlinear case, the design values of strokes and forces at storeys increase and the MAFs of exceedance decrease as expected, but some trends can be observed for what concerns the variations in the r_D and r_F ratios. Generally the values of the ratios at storeys and their maxima increase and the difference is notably larger for the damper forces. The distribution storey by storey is still roughly uniform, with some exceptions for the small values of stroke at upper levels of the 9-storey case.

The discussed trends are confirmed in the Table 5, regarding the stronger extrapolation inherent the factor 200%. In this case the MAFs of exceedance are notably lower but they are still roughly uniform for the linear dampers. The differences between strokes and forces are enhanced and the MAFs of exceedance reduction is more and more large for the forces. Also the differences between the linear and nonlinear case are confirmed and enhanced. The maximum values of r_D are around doubled and larger differences occur for the force ratio r_F.

In general, the observed variations in the MAFs of exceedance are not uniform. By passing from the linear case to the nonlinear case, the simplified approach may provide a different estimation of the reliability regarding the stroke and the forces. A refinement of magnification factors for practical design is desirable, as already implicitly recognized in [2] (*"The increases in force and displacement capacity listed in this standard are based on the judgment of the authors."*), but it obviously requires a deeper investigation and a larger set of case studies.

Table 4. Code design values and MAF of exceedance of the stroke and force of the dampers. Amplification factor 1.30.

Storey	α = 1.00						α = 0.15					
	D_d [m]	v_D [1/yrs]	r_D [-]	F_d [kN]	v_F [1/yrs]	r_F [-]	D_d [m]	v_D [1/yrs]	r_D [-]	F_d [kN]	v_F [1/yrs]	r_F [-]
1	0.092	1.76E-04	0.42	5109	1.13E-04	0.23	0.114	1.83E-04	0.51	2110	3.11E-04	0.27
2	0.104	1.70E-04	0.38	5628	1.01E-04	0.19	0.144	1.89E-04	0.49	2187	5.84E-04	0.35
3	0.073	1.63E-04	0.37	3936	9.80E-05	0.16	0.118	2.30E-04	0.52	2184	6.26E-04	0.48
max			**0.42**			**0.23**			**0.52**			**0.48**

Storey	α = 1.00						α = 0.15					
	D_d [m]	v_D [1/yrs]	r_D [-]	F_d [kN]	v_F [1/yrs]	r_F [-]	D_d [m]	v_D [1/yrs]	r_D [-]	F_d [kN]	v_F [1/yrs]	r_F [-]
1	0.131	1.55E-04	0.42	17623	2.36E-04	0.31	0.156	2.15E-04	0.48	8043	7.04E-04	0.34
2	0.113	1.62E-04	0.45	13675	1.53E-04	0.29	0.131	2.29E-04	0.53	7710	7.51E-04	0.50
3	0.106	1.57E-04	0.44	12331	1.11E-04	0.25	0.114	2.39E-04	0.54	7519	8.85E-04	0.47
4	0.096	1.52E-04	0.42	11662	9.91E-05	0.22	0.093	2.47E-04	0.52	7397	9.89E-04	0.56
5	0.078	1.53E-04	0.40	10408	1.01E-04	0.21	0.061	2.38E-04	0.46	7035	8.26E-04	0.52
6	0.063	1.54E-04	0.38	9223	1.23E-04	0.23	0.040	2.04E-04	0.35	6722	5.45E-04	0.59
7	0.053	1.62E-04	0.36	8280	1.64E-04	0.25	0.029	1.65E-04	0.14	6725	1.58E-04	0.52
8	0.043	1.73E-04	0.36	6979	1.53E-04	0.25	0.026	3.81E-04	0.09	6817	2.73E-05	0.50
9	0.027	1.96E-04	0.40	4854	4.33E-05	0.19	0.024	5.20E-04	0.06	6864	1.90E-10	0.35
max			**0.45**			**0.31**			**0.54**			**0.59**

Table 5. Code design values and MAF of exceedance of the stroke and force of the dampers. Amplification factor 2.00.

Storey	α = 1.00						α = 0.15					
	D_d [m]	v_D [1/yrs]	r_D [-]	F_d [kN]	v_F [1/yrs]	r_F [-]	D_d [m]	v_D [1/yrs]	r_D [-]	F_d [kN]	v_F [1/yrs]	r_F [-]
1	0.142	2.84E-05	0.068	7861	2.88E-06	0.006	0.175	4.81E-05	0.134	2251	1.70E-05	0.015
2	0.160	2.02E-05	0.045	8659	6.79E-07	0.001	0.222	4.48E-05	0.117	2333	6.56E-05	0.039
3	0.113	1.90E-05	0.043	6055	3.97E-07	0.001	0.182	6.13E-05	0.138	2330	1.40E-04	0.108
max			**0.068**			**0.006**			**0.138**			**0.108**

Storey	α = 1.00						α = 0.15					
	D_d [m]	v_D [1/yrs]	r_D [-]	F_d [kN]	v_F [1/yrs]	r_F [-]	D_d [m]	v_D [1/yrs]	r_D [-]	F_d [kN]	v_F [1/yrs]	r_F [-]
1	0.201	3.04E-05	0.081	27113	1.92E-05	0.025	0.239	6.01E-05	0.133	8579	1.22E-04	0.060
2	0.174	3.30E-05	0.091	21038	7.62E-06	0.015	0.202	6.67E-05	0.156	8225	1.74E-04	0.115
3	0.163	3.15E-05	0.088	18971	2.63E-06	0.006	0.176	6.98E-05	0.159	8023	2.36E-04	0.125
4	0.148	2.95E-05	0.081	17941	1.90E-06	0.004	0.143	7.08E-05	0.150	7889	3.05E-04	0.172
5	0.120	2.86E-05	0.074	16013	2.36E-06	0.005	0.093	4.88E-05	0.094	7507	2.46E-04	0.155
6	0.097	2.80E-05	0.068	14189	4.12E-06	0.008	0.061	2.73E-05	0.047	7170	1.61E-04	0.174
7	0.081	2.79E-05	0.062	12738	7.92E-06	0.012	0.045	6.34E-06	0.005	7173	3.38E-05	0.111
8	0.066	3.27E-05	0.068	10737	8.29E-06	0.014	0.040	3.12E-06	0.001	7268	4.02E-06	0.073
9	0.042	4.42E-05	0.091	7467	1.70E-06	0.007	0.037	2.56E-06	0.000	7318	2.48E-12	0.005
max			**0.091**			**0.025**			**0.159**			**0.174**

CONCLUSIONS

This paper analyzes the influence of damper nonlinearity level on the probabilistic seismic performance of building frames equipped with viscous dampers subjected to an uncertain seismic input represented by a set of ground motions scaled to different intensity levels. In particular, a probabilistic methodology is developed to evaluate how the viscous damper exponent α affects the statistics of different response parameters and the seismic performance as measured in terms of

demand hazard curves. A comparison between the deterministic and probabilistic estimates of the seismic demand is carried out by evaluating the performance of families of case studies consisting of frames equipped with dampers with different values of the exponent α designed to ensure the same deterministic performance objective. In particular, a 3-storey and a 9-storey steel building frames are considered as case studies. These two frames are characterized by different dynamic properties and seismic hazard scenarios, described by the seismic intensity im_{ref} and the relevant MAF of exceedance v_{ref}. Global (maximum inter-storey drift, maximum absolute acceleration, base shear) and local (strokes and forces at dampers) demand parameters are reported and discussed.

The main conclusions of the analysis of the case studies are:

- The response statistics (*edp* vs *im*) are notably influenced by the nonlinear exponent α. This influence is different for the various parameters considered and also changes with the seismic intensity level. These differences in the response reflect on the demand hazard (v vs *edp*) and quite similar qualitative trends have been observed for the case studies and seismic scenarios considered.

- The probabilistic seismic demand corresponding to the reference value of MAF of exceedance v_{ref} is higher than the deterministic design demand for all the observed parameters. The difference between the two values reflects the dispersion of the response due to record-to-record variability, which is different for the different *EDP*s and α levels considered.

- The demands corresponding to target values of the MAF of exceedance different from v_{ref} also show trends depending strongly on α. The relationship between the damper force demand and the logarithm of the MAF of exceedance is essentially linear for both the case studies and for all the values of the nonlinear parameters α. This relationship is less than linearly proportional for the base shear and it is more than linearly proportional for the inter-storey drifts, damper strokes and absolute accelerations.

- In the final part of the paper, the analysis results are employed to evaluate the reliability of simplified approaches usually adopted in codes of practice for the damper design. These approaches generally magnify the deterministic results coming from the structural analysis to estimate values of the demand to be used for the reliability assessment. Application of the probabilistic results to the case studies showed some limits of this approach and, in particular, showed that not uniform differences in the MAF of exceedance arise by passing from the linear case to the nonlinear case.

Magnification factors for the demand estimates should consider the nonlinear parameter α and further investigations encompassing different damper distributions, seismic input properties and added damping levels are necessary to provide more reliable approximated formulas.

ACKNOWLEDGEMENT

REFERENCES

[1]   FEMA-445. Next-Generation Performance-Based Seismic Design Guidelines, Washington DC, 2006.

[2]   ASCE 41-06. Seismic Rehabilitation of Existing Buildings. American Society of Civil Engineers, Reston, Virginia, 2007.

[3]   European Committee for Standardization. Eurocode 8—Design of Structures for Earthquake Resistance. Part 1: General Rules, Seismic Actions and Rules for Buildings, Brussels, Belgium, 2004.

[4]   Constantinou MC, Whittaker AS, Kalpakidis Y, Fenz DM, Warn GP. Performance of Seismic Isolation Hardware under Service and Seismic Loading. Technical Report MCEER-

07-0012, Multidisciplinary Center for Earthquake Engineering Research, State University of New York at Buffalo, Buffalo, NY, USA, 2008.

[5] Soong TT, Dargush GF. Passive Energy Dissipation Systems in Structural Engineering. Wiley: New York, 1997.

[6] Christopoulos C, Filiatrault A. *Principles of Passive Supplemental Damping and Seismic Isolation*. IUSS Press: Pavia, Italy, 2006.

[7] Lavan O, Dargush GF. Multi-Objective Evolutionary Seismic Design with Passive Energy Dissipation Systems, *Journal of Earthquake Engineering* 2009; **13**(6): 758-790.

[8] Pavlou E, Constantinou MC. Response of Nonstructural Components in Structures with Damping Systems. *Journal of Structural Engineering* 2006; **132**(7); 1108-1117.

[9] Castellano MG, Borrella R, Infanti S, Gattulli V. Experimental characterization of nonlinear fluid viscous dampers according to the New European Standard. *Proceedings of EACS 2012, 5th European Conference on Structural Control*. Genoa, Italy, 18-20 June 2012.

[10] Peckan G, Mander JB, Chen SS. Fundamental Considerations for the design of non-linear viscous dampers. *Earthquake Engineering and Structural Dynamics* 1999; **28**(11): 1405-1425.

[11] Lin WH, Chopra AK. Earthquake response of elastic SDF systems with non-linear fluid viscous dampers. *Earthquake Engineering and Structural Dynamics* 2002; **31**(9): 1623-1642.

[12] Martinez-Rodrigo M, Romero ML. An optimum retrofit strategy for moment resisting frames with nonlinear viscous dampers for seismic applications. *Engineering Structures* 2003; **25**(7): 913–925.

[13] Goel RK. Seismic response of linear and non-linear asymmetric systems with non-linear fluid viscous dampers. *Earthquake Engineering and Structural Dynamics* 2005; **34**(7): 825–846. DOI: 10.1002/eqe.459

[14] Bahnasy A, Lavan O. Linear or Nonlinear Fluid Viscous Dampers? A Seismic Point of View. *Proceedings of the Structures Congress*, Pittsburgh, 2013.

[15] Dicleli M, Mehta A. Effect of near-fault ground motion and damper characteristics on the seismic performance of chevron braced steel frames. *Earthquake Engineering and Structural Dynamics* 2007; **36**(7):927–948.

[16] FEMA-368. NEHRP recommended provisions for seismic regulations for new buildings and other structures, 2000 Edition, Part 1, Washington DC, 2000.

[17] NZS 1170.5. Structural design actions, Part 5: Earthquake actions - New Zealand. New Zealand Standards, Wellington, NZ, 2004.

[18] American Society of Civil Engineers (ASCE). *Minimum design loads for buildings and other structures*, Reston, VA, 2006.

[19] Bradley BA. A comparison of intensity-based demand distributions and the seismic demand hazard for seismic performance assessment. *Earthquake Engineering and Structural Dynamics* 2013; **42**(15): 2235-2253.

[20] Güneyisi EM, Altay G. Seismic fragility assessment of effectiveness of viscous dampers in R/C buildings under scenario earthquakes. *Structural Safety* 2008; **30**(5): 461-480.

[21] Barroso LR. Performance evaluation of vibration controlled steel structures under seismic loads. PhD thesis, Stanford University, California, US, 1999.

[22] Barroso LR, Winterstein S. Probabilistic seismic demand analysis of controlled steel moment-resisting frame structures. *Earthquake Engineering and Structural Dynamics* 2002; **31**(12): 2049-2066.

[23] Wanitkorkul A, Filiatrault A. Influence of Passive Supplemental Damping Systems on

Structural and Nonstructural Seismic Fragilities of a Steel Building. *Engineering Structures* 2008; **30**(3): 675-682.

[24] Seo CY, Karavasilis TL, Ricles JM, Sause R. Seismic performance and probabilistic collapse resistance assessment of steel moment resisting frames with fluid viscous dampers, *Earthquake Engineering and Structural Dynamics* 2014; **43**(14): 2135-2154.

[25] Gidaris I, Taflanidis AA. Performance assessment and optimization of fluid viscous dampers through life-cycle cost criteria and comparison to alternative design approaches, *Bulletin of Earthquake Engineering* 2015; **13**:1003-1028.

[26] Shin H, Singh MP. Minimum failure cost-based energy dissipation system designs for buildings in three seismic regions – Part II: Application to viscous dampers*, Engineering Structures* 2014; **74**: 275-282.

[27] Di Paola M, Mendola LL, Navarra, G. Stochastic seismic analysis of structures with nonlinear viscous dampers. *Journal of Structural Engineering* 2007; **133**(10): 1475-1478.

[28] Di Paola M, Navarra G. Stochastic seismic analysis of MDOF structures with nonlinear viscous dampers. *Structural Control and Health Monitoring* 2009, **16**(3): 303-318.

[29] Tubaldi E, Barbato M, Dall'Asta A. Performance-based seismic risk assessment for buildings equipped with linear and nonlinear viscous dampers 2014, *Engineering Structures*; 78: 90-99.

[30] Tubaldi E, Ragni L, Dall'Asta A. Probabilistic seismic response assessment of linear systems equipped with nonlinear viscous dampers, *Earthquake Engineering and Structural Dynamics* 2014; DOI: 10.1002/eqe.2461.

[31] Tubaldi E, Kougioumtzoglou IA. Nonstationary stochastic response of structural systems equipped with nonlinear viscous dampers under seismic excitation. *Earthquake Engineering and Structural Dynamics* 2014; DOI: 10.1002/eqe.2462.

[32] Ohtori Y, Christenson RE, Spencer Jr. BF, Dyke SJ. Benchmark Control Problems for Seismically Excited Nonlinear Buildings. *Journal of Engineering Mechanics* 2004; **130**(4): 366–385.

[33] Lavan, O., & Avishur, M. Seismic behavior of viscously damped yielding frames under structural and damping uncertainties. *Bulletin of Earthquake Engineering* 2013; **11**(6): 2309-2332.

[34] Politopoulos I, Sollogoub P. Vulnerability of elastomeric bearing isolated buildings and their equipment. *Journal of earthquake engineering* 2005; **9**(04): 525-546.

[35] Politopoulos I, Pham HK. Sensitivity of seismically isolated structures. *Earthquake Engineering and Structural Dynamics* 2009; **38**(8), 989-1007.

[36] Jalayer F, Cornell CA. Alternative non-linear demand estimation methods for probability-based seismic assessments. *Earthquake Engineering and Structural Dynamics* 2009; **38**(8): 951–972.

[37] Luco N, Cornell CA. Structure-specific scalar intensity measures for near-source and ordinary earthquake ground motions. *Earthquake Spectra* 2007; **23**(2): 357-92.

[38] Aslani H, Miranda E. Probability-based seismic response analysis. Engineering Structures 2005; **27**(8): 1151-1163.

[39] JCSS. *Probabilistic Model Code: Part 1: Basis of Design*. Joint Committee on Structural Safety, 2000.

[40] European Committee for Standardization. *Eurocode 0 - Basis of structural design*. Brussels, Belgium, 2002.

[41] McKenna F, Fenves GL, Scott MH. *OpenSees: open system for earthquake engineering simulation*. Pacific Earthquake Engineering Center, University of California, Berkeley, CA

2006.

[42] Whittle JK, Williams MS, Karavasilis TL, Blakeborough A. Comparison of Viscous Damper Placement Methods for Improving Seismic Building Design, *Journal of Earthquake Engineering* 2012; **16**(4): 540-560

[43] Hwang JS, Lin WC, Wu NJ. Comparison of distribution methods for viscous damping coefficients to buildings, *Structure and Infrastructure Engineering: Maintenance, Management, Life-Cycle Design and Performance* 2013; 9(1):28-41.

[44] Freddi F, Tubaldi E, Ragni L, Dall'Asta A. Probabilistic performance assessment of low-ductility RC frames retrofitted with dissipative braces. *Earthquake Engineering and Structural Dynamics* 2013; **42**(7): 993-1011.

[45] Zona A, Ragni L, Dall'Asta A. Sensitivity-based study of the influence of brace over-strength distribution on the seismic response of steel frames with BRBs. *Engineering Structures* 2012; **37**: 179-192.

[46] Landi L, Diotallevi P, Castellari G. On the Design of Viscous Dampers for the Rehabilitation of Plan-Asymmetric Buildings. *Journal of Earthquake Engineering* 2013; **17**(8): 1141-1161.

[47] FEMA-274. NEHRP Commentary on the Guidelines for the Seismic Rehabilitation of Buildings. Federal Emergency Management Agency, Washington DC, 1997.